

A LASER BEAM INDUCED OPTICAL MANIPULATION OF A SMECTITE

Yuki HIGASHI^a, Takashi NAGASHITA^a, Teruyuki NAKATO^b,
Yasutaka SUZUKI^a, and Jun KAWAMATA^{a,*}

^aGraduate School of Science and Technology for Innovation, Yamaguchi University,
Yamaguchi 753–8512, Japan

^bDepartment of Applied Chemistry, Kyushu Institute of Technology, Kitakyushu 804–8550, Japan

(Received September 14, 2018. Accepted September 20, 2018)

ABSTRACT

On-demand and local manipulation of exfoliated clay nanosheets in colloidal dispersions enables a variety of novel applications of clay-based materials. In this study, manipulation of a single fluorohectorite nanosheet by utilizing the radiation pressure of a tightly focused laser beam was demonstrated. When a linearly polarized continuous laser beam was irradiated to a fluorohectorite nanosheet, the nanosheet was oriented with its in-plane direction parallel to the propagation direction of the laser beam. Furthermore, the nanosheet edge was directed in parallel to the polarization direction of the laser beam. When the polarization direction of the laser beam was rotated, the nanosheet was rotated following the rotation of the polarization direction.

Key words: optical manipulation, radiation pressure, fluorohectorite, nanosheet, colloid

INTRODUCTION

Layered crystals such as clay minerals can be exfoliated into single nanosheets in an aqueous medium, which results in colloidal nanosheets. The colloidal nanosheets can be oriented by a shear force, electric field, or magnetic field (Schmidt *et al.*, 2002; Sasai *et al.*, 1996; de Azevedo *et al.*, 2007). Various macroscale structures have also been organized from colloidal nanosheets with these external forces (Nakato *et al.*, 2011; Schmidt *et al.*, 2002; Sasai *et al.*, 1996; Azevedo *et al.*, 2007). If on-demand and microscale orientation control of colloidal nanosheets is realized, a variety of hierarchical colloidal structures, which are not obtained by macroscopic external forces, will be formed.

A colloidal particle can be trapped at a focal point when a tightly focused laser beam is irradiated to the particle (Ashkin, 1992; Harada and Asakura, 1996). When a photon is reflected or refracted by a particle, its momentum changes. Based on the conservation of momentum, a reactive force corresponding to the momentum change is applied to the particle. This force is called “radiation pressure.” The radiation pressure is consisting of two major forces: scattering and gradient forces. Origin of the scattering force is reflection of a

photon. This force pushes the particle toward the propagation direction of the incident beam. Gradient force is mainly from refraction of the focused beam. This force drags the particle toward the focal point of the incident beam. When these two forces are appropriately balanced, a particle in colloid can be trapped at the focal point of the incident beam.

We have realized local and on-demand orientation of a colloidal hexaniobate ($K_4Nb_6O_{17}$) nanosheet by irradiation of a focused laser beam (Tominaga *et al.*, 2018a; Nagashita *et al.*, 2018). The niobate nanosheet was oriented parallel to both of the propagation and polarization directions of the incident linearly polarized laser beam when the niobate nanosheet was trapped at the focal point. Since the dominant origins of radiation pressure are reflection and refraction, the radiation pressure is large when the difference of refractive indexes between dispersion medium and dispersoid is large. Because hexaniobate $K_4Nb_6O_{17}$ is known as an oxide exhibiting a high refractive index around 2.3 (Nassau *et al.*, 1969), its nanosheet is favorable for optical manipulation. However, this material possesses photocatalytic activity (Domen *et al.*, 1986, 2000). Thus, organic molecules adsorbed on niobate nanosheet are often photodecomposed (Umemura *et al.*, 2006; Shinozaki and Nakato, 2007; Sarahan *et al.*, 2008). Therefore, niobate nanosheet is not appropriate as a host material of organic compounds to limit their application for functional inorganic–organic hybrids.

In contrast, organic molecules can be adsorbed stably onto the surface of clay minerals because most of clay minerals do not exhibit photocatalytic activity (Olphene, 1966; Umemu-

*Corresponding author: Jun Kawamata, Graduate School of Science and Technology for Innovation, Yamaguchi University, Yamaguchi 753–8512, Japan. e-mail: j_kawa@yamaguchi-u.ac.jp

ra, 2004). Therefore, clay minerals are suitable host material of photo- and optical-functional hybrid materials. In fact, clay mineral nanosheets have been utilized as host materials of photo- and optical-functional organic molecules (Cenens and Schoonheydt, 1988; Ogawa and Kuroda, 1995; Salleres *et al.*, 2009; Sasai *et al.*, 2009; Bujdák *et al.*, 2010; Takagi *et al.*, 2010; Kawamata *et al.*, 2010; Dutta *et al.*, 2012; Suzuki *et al.*, 2012; Nakato *et al.*, 2017). This is because most of clay mineral nanosheets are colorless and transparent in the visible wavelength region and thereby interactions between the guest organic molecules and incident light are not disturbed by the host materials. Photo- and optical-functions of organic molecules adsorbed on clay nanosheets are often different from those in solution or pure solid states. Dyes adsorbed on clay nanosheets often show large spectral shift and high photoluminescence quantum yield compared with those in a homogeneous solution (Okahata *et al.*, 1989; Ishida *et al.*, 2014). Two-photon absorption properties of organic molecules adsorbed on a clay have significantly been improved (Suzuki *et al.*, 2011). Moreover, such photo- and optical-functions are controlled by nanosheet orientation (Sasai *et al.*, 2004; Bujdák *et al.*, 2005). Thus, on-demand and hierarchical orientation control of clay-organic hybrid nanosheets may further improve their functionalities.

However, typical refractive index of a clay mineral is reported to be about 1.5 (Querry, 1987; The Clay Science Society of Japan, 1987). Due to this low refractive index, conditions for optical manipulation of clay mineral nanosheets

should be different from those of niobate nanosheet. Thus, in this study, optical manipulation behaviors of an exfoliated clay mineral, fluorohectorite, has been investigated.

MATERIALS AND METHODS

Synthetic fluorohectorite provided from Topy Industries, Ltd., Japan, was used in this study. Prior to the optical manipulation, it was purified as follows. Powder sample of fluorohectorite was dispersed in ultra pure water with a concentration of 5 g L^{-1} , and then centrifuged at 15000rpm for 15 min. After decantation, the resulting supernatant was again centrifuged at 15000rpm for 15 min. Centrifugation was repeated for several times until the precipitate was judged to be colorless. The resulting supernatant was freeze-dried.

A fluorohectorite nanosheet colloid used for optical manipulation was prepared by adding the purified clay powder to water at a concentration of 0.01 g L^{-1} . This concentration is sufficient to exfoliate the clay mineral into single layers (Kawamata *et al.*, 2010). The colloid sample was injected into a $100 \mu\text{m}$ thick thin-layer glass cell. The cell was set on the stage of an inverted microscope (IX70, Olympus, Japan). Figure 1 shows a schematic representation of the experimental setup. A linearly polarized continuous-wave laser beam emitting at 532 nm (Millennia Pro, Spectra Physics, USA) was focused at the center of the cell ($50 \mu\text{m}$ from the cell-sample interface) using an objective lens (Apo, $60\times$, numerical aperture = 1.20, Olympus, Japan). The polarization direction of the linearly polarized laser beam with respect to the sample was varied by rotating a half-wave plate mounted on a stepper motor. The beam diameter was adjusted to the pupil diameter of the objective lens using a beam expander. The beam waist at the focal point of this setup was calculated to be $0.33 \mu\text{m}$.

For optical microscopy observation upon irradiation with a laser beam, the sample was illuminated by a halogen lamp and the image was monitored with a digital C-MOS camera (ORCA-Flash 4.0 V3, Hamamatsu Photonics). The incident laser beam was completely blocked by a dichroic mirror and a band pass filter inserted before the camera. Theoretical spatial resolutions and the depth of field in the experimental setup were approximately $0.3 \mu\text{m}$, which was 0.3% of the thickness of the cell.

RESULTS

The optical microscope images of the fluorohectorite colloid before and after irradiation with the linearly polarized laser beam are shown in Figure 2. A plate-like object is ob-

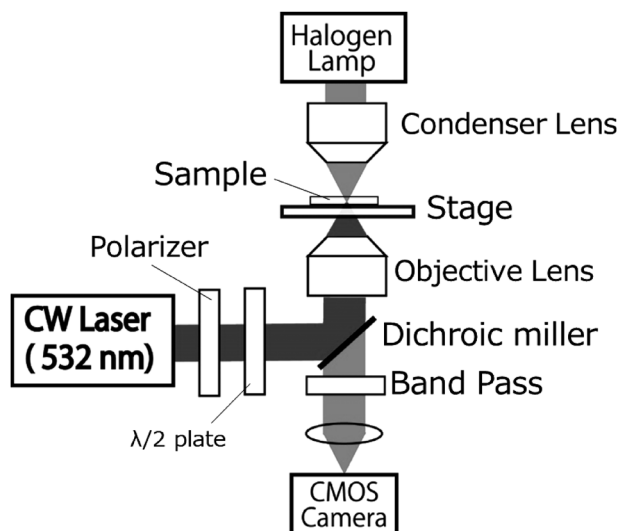


Fig. 1. Schematic representation of experimental setup used for laser manipulation of fluorohectorite nanosheet.

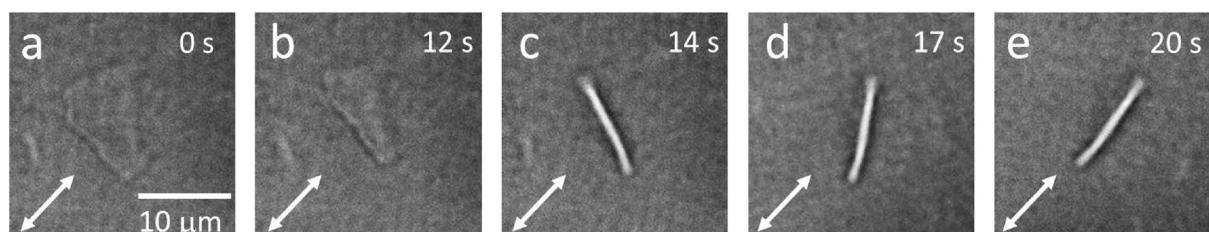


Fig. 2. Optical microscope images of a fluorohectorite nanosheet before and after laser irradiation. The white arrow indicates the polarization direction.

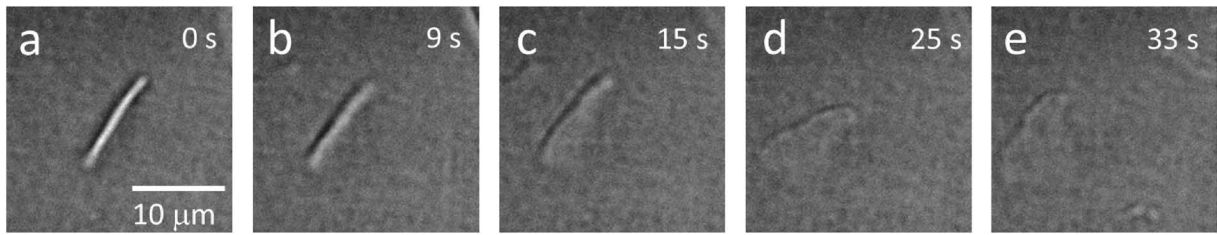


Fig. 3. Optical microscope images of a fluorohectorite nanosheet after laser irradiation ceases.

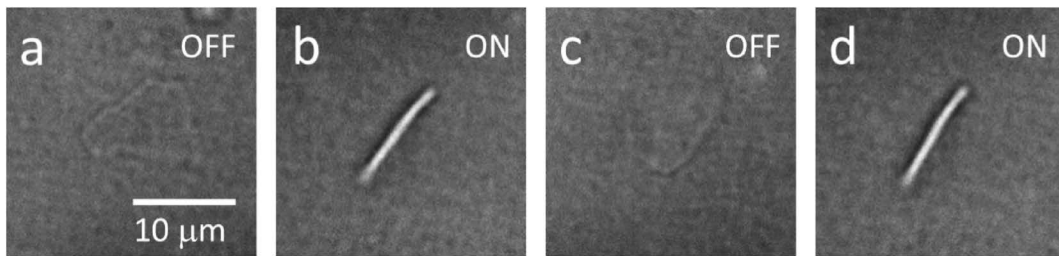


Fig. 4. Optical microscope image of the repeatedly trapped fluorohectorite nanosheet by on-off switching of the laser irradiation. Before laser irradiation (a), after 30 s of continuous laser irradiation (b), 30 s after laser irradiation ceased (c) and after 30 s re-irradiation of continuous laser beam (d).

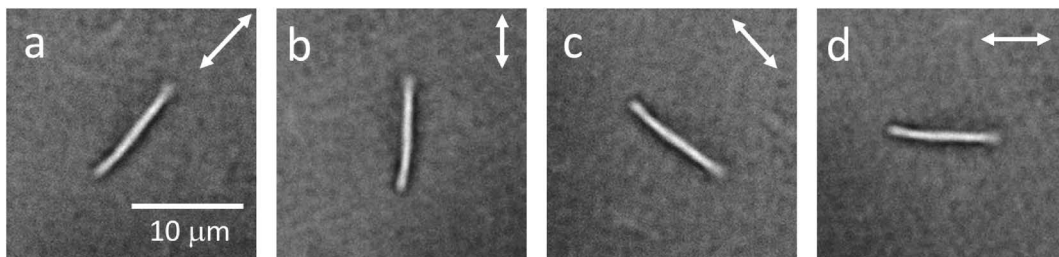


Fig. 5. Optical microscope images of a fluorohectorite nanosheet when polarized laser beam with various polarization direction was irradiated. The white arrows indicate the polarization directions.

served before laser irradiation (Figure 2a). This object was assigned to a fluorohectorite nanosheet oriented with their in-plane direction parallel to the cell surface. The nanosheet moved three-dimensionally with Brownian motion; thus, the object was sometimes clearly seen but sometimes blurred with focusing and de-focusing in microscope observations due to the motion. The area of in-plane direction of the nanosheet estimated by the microscope image under the assumption that the nanosheet is perfectly parallel to the cell surface was $97 \mu\text{m}^2$.

With the irradiation of a 50 mW of laser beam, the nanosheet was immediately trapped at around the focal point. After 12 s of continuous laser irradiation, the fluorohectorite nanosheet started tilting toward the direction perpendicular to the cell surface, i.e., parallel to the propagation direction of the laser beam (Figure 2b). After 14 s, the fluorohectorite nanosheet was stationarily oriented in this direction (Figure 2c). Then, the oriented nanosheet started rotation of its edge with respect to the laser propagation direction (Figure 2d, 17 s). The final direction of the nanosheet edge was parallel to the polarization direction of the incident laser beam. The nanosheet retained the trapped state during laser irradiation (Figure 2e, 22 s).

The fluorohectorite nanosheet was gradually relaxed by Brownian motion when the laser irradiation was ceased

(Figure 3). The nanosheet trapped at the focal point began positional and orientational shift just after stopping the laser irradiation (Figure 3a). The object was then gradually moved and tilted into the direction parallel to the cell surface (Figure 3b–e).

The fluorohectorite nanosheet was repeatedly trapped at the focal point by on-off switching of the laser irradiation, as shown in Figure 4. Figures 4a to 4c show trapping and releasing cycle described above. The released nanosheet (Figure 4c) was re-trapped at the focal point again by re-irradiation of continuous laser beam (Figure 4d). The trapping and releasing was repeated by further on-off switching cycles of the laser irradiation at least 10 times.

Figure 5 shows that the fluorohectorite nanosheet was rotated following the polarization direction of the incident laser beam. At the initial stage, a nanosheet was trapped in the diagonal direction in the microscope image by irradiation of a laser beam linearly polarized in this direction (Figure 5a). When the polarization direction was rotated clockwise by 45° , the fluorohectorite was also rotated clockwise by 45° (Figure 5b). When the polarization direction was sequentially further rotated by 45° , the nanosheet followed the rotation of the polarization direction (Figures 5c and d). Rotation of the nanosheet was followed until the maximum speed of stepper motor of our experimental set up of $0.5 \pi \text{ rad s}^{-1}$.

DISCUSSION

Our results demonstrate that fluorohectorite nanosheets are manipulated by a laser beam. As shown in Figure 2, when a continuous laser beam was irradiated to a fluorohectorite nanosheet, in-plane direction of the nanosheet changed from parallel to perpendicular to the cell surface. Namely, resulted direction of the nanosheet surface was parallel to the propagation direction of the laser beam. Furthermore, the nanosheet was rotated to the direction of its edge in parallel to the polarization direction of the laser beam. This behavior was essentially the same as the case of niobate nanosheet (Tomimaga *et al.*, 2018a). Responses of fluorohectorite nanosheet to laser irradiation shown in Figure 3–5 were also essentially the same as those observed for niobate nanosheet except for the required laser power. At least 50 mW of laser power was required for obtaining orientation change of $97 \mu\text{m}^2$ of fluorohectorite nanosheet while the power for $102 \mu\text{m}^2$ of niobate nanosheet was 5 mW, in our experimental setup. Thus, the laser power required for manipulating fluorohectorite nanosheet was much higher than that for niobate nanosheet. The higher laser power required for trapping fluorohectorite nanosheet can be attributed to the small refractive index of fluorohectorite because areas of in-plane direction of the fluorohectorite and the niobate nanosheet were almost same value. It should be noted here that fluorohectorite nanosheet was not damaged even though such a large intensity of laser beam was irradiated. Although a large laser power is required, this study clearly indicated that clay nanosheet in colloidal dispersion can also be optically manipulated by a focused laser beam, as well as niobate nanosheet.

A nanosheet oriented parallel to the propagation direction of incident laser beam was observed as a linear object. The thickness of the observed linear object seems to be around 900 nm in the microscope images. However, the thickness of exfoliated fluorohectorite nanosheet is 0.95 nm. The most probable reason for this discrepancy is the considerably larger lateral size (5 to $20 \mu\text{m}$) of the trapped fluorohectorite compared to the Rayleigh length ($0.3 \mu\text{m}$) of the objective lens employed in this study. Since the Rayleigh length, i.e., focal depth, is significantly smaller than the lateral size of nanosheet both edges of the nanosheet are located far from the focal depth of the objective lens, when the nanosheet is oriented with its in-plane direction parallel to the propagation direction of the laser beam and the focal depth is set to the center of nanosheet. Thus, image of the edges should be blurred. Due to this defocusing of the edges, the single nanosheet was thought to be observed as if such a thick object.

CONCLUSIONS

In this study, we have demonstrated laser manipulation of a single clay nanosheet. Reflecting a relatively small refractive index of clay minerals, required laser power was larger than those for oxide nanosheets with high refractive indexes. Methodologies that enable local and on-demand orientation manipulation of clay minerals nanosheets is needed for maximizing the functionality of clay-dye hybrids, and optical manipulation established in this study should provide a powerful

methodology for realizing required orientations of clay mineral nanosheets. Novel practical applications toward superior optical properties of clay-dye hybrids will also be found under appropriate manipulation.

ACKNOWLEDGEMENTS

The authors would like to thank to Dr. Makoto Tomimaga (University of Bayreuth) for valuable advices throughout this study. We gratefully acknowledge Ms. Ayaka Yoshida and Mr. Akira Ikeda (Yamaguchi University) for their supports to sample purification. This work was supported by JSPS KAKENHI Grant Numbers 15H03878 (T.N.), 17H05466 (Y.S.) and 15K13676 (J.K.). Y.H. is thankful for support from the Clay Science Society of Japan.

REFERENCES

- ASHKIN, A. (1992) Forces of a single-beam gradient laser trap on a dielectric sphere in the ray optics regime. *Biophysical Journal*, **61**, 569–582.
- BUJDAK, J. and IYI, N. (2005) Molecular orientation of rhodamine dyes on surfaces of layered silicates. *The Journal of Physical Chemistry B*, **109**, 4608–4615.
- BUJDAK, J., CHORVAT, D. Jr., and IYI, N. (2010) Resonance energy transfer between rhodamine molecules adsorbed on layered silicate particles. *The Journal of Physical Chemistry C*, **114**, 1246–1252.
- CENENS, J. and SCHOONHEYDT, R.A. (1988) Visible spectroscopy of methylene blue on hectorite, laponite b, and barasym in aqueous suspension. *Clays and Clay Minerals*, **36**, 214–224.
- DE AZEVEDO, E.N., ENGELSBURG, M., FOSSUM, J.O., and DE SOUZA, R.E. (2007) Anisotropic water diffusion in nematic self-Assemblies of clay nanoplatelets suspended in water. *Langmuir*, **23**, 5100–5105.
- DOMEN, K., KUDO, A., SHINOZAKI, A., TANAKA, A., MARUYA, K., and ONISHI, T. (1986) Photodecomposition of water and hydrogen evolution from aqueous methanol solution over novel niobate photocatalysts. *Journal of the Chemical Society Chemical communications*, **4**, 356–357.
- DOMEN, K., KONDO, J., HARA, M., and TAKATA, T. (2000) Photo- and mechano-Catalytic overall water splitting reactions to form hydrogen and oxygen on heterogeneous catalysts. *Bulletin of the Chemical Society of Japan*, **73**, 1307–1331.
- DREGER, Z.A. and DRICKAMER, H.G. (1997) Effect of environment on pressure-Induced emission of benzophenone, 4,4'-dichlorobenzophenone, and 4-(dimethylamino)benzaldehyde in solid media. *The Journal of Physical Chemistry A*, **101**, 1422–1428.
- DREGER, Z.A., WHITE, J.O., and DRICKAMER, H.G. (1998) High pressure-controlled intramolecular-twist of flexible molecules in solid polymers. *Chemical Physics Letters*, **290**, 399–404.
- DUTTA, D. and VASUDEVAN, S. (2012) Accommodating unwelcome guests in inorganic layered hosts: inclusion of chloranil in a layered double hydroxide. *Inorganic Chemistry*, **51**, 8064–8072.
- HARADA, Y. and ASAKURA, T. (1996) Radiation forces on a dielectric sphere in the Rayleigh scattering regime. *Optics Communications*, **124**, 529–541.
- ISHIDA, Y., SHIMADA, T., and TAKAGI, S. (2014) "Surface-fixation induced emission" of porphyrine dye by a complexation with inorganic nanosheets. *The Journal of Physical Chemistry C*, **118**, 20466–20471.
- KAWAMATA, J., SUZUKI, S., and TENMA, Y. (2010) Fabrication of clay mineral-dye composites as nonlinear optical materials. *Philosophical Magazine*, **90**, 2519–2527.
- MIYAMOTO, N., KURODA, K., and OGAWA, M. (2004) Visible light induced electron transfer and long-lived charge separated state in cyanine dye/Layered titanate intercalation compounds. *The Journal of Physical Chemistry B*, **108**, 4268–4274.
- NAGASHITA, T., HIGASHI, Y., IKEDA, A., TOMINAGA, M., KUMAMOTO, T., SUZUKI, Y., NAKATO, T., and KAWAMATA, J. (2018) Laser beam induced orientation control of a nanosheet liquid crystal by employing an objective lens with a low numerical aperture. *Clay Science*, **22**, 13–17.
- NAKATO, T., KAWAMATA, J., and TAKAGI, S. ed. (2017) *Inorganic Nanosheets and Nanosheet-Based Materials*, pp. 474–479, Springer, Basel.

- NAKATO, T., KURODA, K., and KATO, C. (1992) Syntheses of intercalation compounds of layered niobates with methylviologen and their photochemical behavior. *Chemistry of Materials*, **4**, 128–132.
- NAKATO, T., NAKAMURA, K., SHIMADA, Y., SHIDO, Y., HOURYU, T., IMURA, Y., and MIYATA, H. (2011) Electrooptic response of colloidal liquid crystals of inorganic oxide nanosheets prepared by exfoliation of a layered niobate. *The Journal of Physical Chemistry C*, **115**, 8934–8939.
- NASSAU, K., SHIEVER, J.W., and BERNSTEIN, J.L. (1969) Crystal growth and properties of mica-like potassium niobates. *Journal of the Electrochemical Society*, **116**, 348–353.
- OGAWA, M. and KURODA, K. (1995) Photofunctions of intercalation compounds. *Chemical Reviews*, **95**, 399–438.
- OKAHATA, Y. and SHIMIZU, A. (1989) Preparation of bilayer-intercalated clay films and permeation control responding to temperature, electric field, and ambient pH changes. *Langmuir*, **5**, 954–959.
- OLPHEN, H.V. (1966) Maya blue: a clay-organic pigment? *Science*, **154**, 645–646.
- SAHARAN, M.C., CARROLL, E.C., ALLEN, M., LARSEN, D.S., BROWNIG, N.D., and OSTERLOH, F.E. (2008) K4Nb6O17-derived photocatalysts for hydrogen evolution from water: nanoscrolls versus nanosheets. *Journal of Solid State Chemistry*, **181**, 1678–1683.
- SALLERES, S., ALBELOA, F.L., MARTINEZ, V., ARBELOA, T., and ARBEROA, I.L. (2009) Photophysics of rhodamine 6G laser dye in ordered surfactant (C12TMA)/clay (Laponite) hybrid films. *The Journal of Physical Chemistry C*, **113**, 965–970.
- SASAI, R., IKUTA, N., and YAMAOKA, K. (1996) Reversing-pulse electric birefringence of montmorillonite particles suspended in aqueous media. Instrumentation and the effect of particle concentration, ionic strength, and valence of electrolyte on field orientation. *The Journal of Physical Chemistry*, **100**, 17266–17275.
- SASAI, R., IYI, N., FUJITA, T., ALBELOA, F.L., TAKAGI, K., and ITOH, H. (2004) Luminescence properties of rhodamine 6G intercalated in surfactant/clay hybrid thin solid films. *Langmuir*, **20**, 4715–4719.
- SASAI, R., ITOH, T., OHMORI, W., ITOH, H., and KUSUNOKI, M. (2009) Preparation and characterization of rhodamine 6G/alkyltrimethylammonium/laponite hybrid solid materials with higher emission quantum yield. *The Journal of Physical Chemistry C*, **113**, 415–421.
- SCHMIDT, G., NAKATANI, A.I., BUTLER, P.D., and HAN, C.C. (2002) Rheology and flow-birefringence from viscoelastic polymer–clay solutions. *Macromolecules*, **41**, 45–54.
- SHINOZAKI, R. and NAKATO, T. (2007) Photochemical behavior of rhodamine 6G dye intercalated in photocatalytically active layered hexaniobate. *Microporous and Mesoporous Materials*, **113**, 81–89.
- SUZUKI, Y., TENMA, Y., NISHIOKA, Y., KAMADA, K., OHTA, K., and KAWAMATA, J. (2011) Efficient two-photon absorption materials consisting of cationic dyes and clay minerals. *The Journal of Physical Chemistry C*, **115**, 20653–20661.
- SUZUKI, Y., TENMA, Y., NISHIOKA, Y., and KAWAMATA, J. (2012) Efficient non-linear optical properties of dyes confined in interlayer nanospaces of clay minerals. *An Asian Journal*, **7**, 1170–1179.
- TAKAGI, S., SHIMADA, T., MASUI, D., TACHIBANA, H., ISHIDA, Y., TYRCK, D., and INOUE, H. (2010) Unique solvatochromism of a membrane composed of a cationic porphyrin–clay complex. *Langmuir*, **26**, 4639–4641.
- THE CLAY SCIENCE SOCIETY OF JAPAN ed. (1987) *Handbook of Clays and Clay Minerals*, 2nd ed., pp. 480–484, Gihodo Shuppan, Tokyo. (Japanese)
- TOMINAGA, M., HIGASHI, Y., KUMAMOTO, T., NAGASHITA, T., NAKATO, T., SUZUKI, Y., and KAWAMATA, J. (2018a) Optical trapping and orientation manipulation of 2D inorganic materials using a linearly polarized laser beam. *Clays and Clay Minerals*, **66**, 138–145.
- TOMINAGA, M., NAGASHITA, T., KUMAMOTO, T., HIGASHI, Y., IWAI, T., NAKATO, T., SUZUKI, Y., and KAWAMATA, J. (2018b) Radiation pressure induced hierarchical structure of liquid crystalline inorganic nanosheets. *ACS Photonics*, **5**, 1288–1293.
- UMEMURA, Y., EINAGA, Y., and YAMAGISHI, A. (2004) Formation of a stable thin sheet of prussian blue in a clay-organic hybrid film. *Materials Letters*, **58**, 2472–2475.
- UMEMURA, Y., SHINOHARA, E., KOURA, A., NISHIOKA, T., and SASAKI, T. (2006) Photocatalytic decomposition of an alkylammonium cation in a langmuir–Blodgett film of a titania nanosheet. *Langmuir*, **22**, 3870–3877.

(Manuscript handled by Kazuhiro Shikinaka)